Int. J. Electrochem. Sci., 15 **(2020)** 9554 – 9567, doi: 10.20964/2020.10.53

International Journal of
ELECTROCHEMICAL
SCIENCE
www.electrochemsci.org

Transition Metal (M = Rh and Ta) Effects on the Electrical Properties and AC Susceptibility of $Tl_{0.85}Cr_{0.15}Sr_{2-x}M_xCaCu_2O_7$ Superconductor

M. S. Mohd-Syahmi, K. Muhammad-Aizat, R. Abd-Shukor[*]

Department of Applied Physics, Universiti Kebangsaan Malaysia, 43600 Bangi, Selangor, Malaysia
[*]E-mail: ras@ukm.edu.my

Received: 29 May 2020 / *Accepted:* 31 July 2020 / *Published:* 31 August 2020

The effects of transition metal (M = Rh and Ta) on $Tl_{0.85}Cr_{0.15}Sr_{2-x}M_xCaCu_2O_7$ (Tl-1212) superconductor for $x = 0 – 0.04$ (M = Rh) and $x = 0 – 0.30$ (M = Ta) were studied. X-ray diffraction patterns showed Tl-1212, Tl-1201 and $Ca_{0.3}Sr_{07}CuO_2$ phases in the samples. Scanning electron micrographs (SEM) showed that the grain size decreased with Rh. The transition temperature increased when Rh and Ta were substituted for low levels. AC susceptibility measurements showed the highest transition temperature $T_{c\chi'} = 98$ K for Rh ($x = 0.02$) and 96 K for Ta ($x = 0.3$) samples. The peak temperature, T_p of the imaginary susceptibility χ'' was the highest for Rh with $x = 0.02$ ($T_p = 93$ K) and Ta with $x = 0.30$ ($T_p = 91$ K). Rh and Ta improved the onset transition temperature of $Tl_{0.85}Cr_{0.15}Sr_{2-x}M_xCaCu_2O_7$ from 97 K to 103 K and 104 K, respectively.

Keywords: transition metal; Tl-1212 phase; AC susceptibility

1. INTRODUCTION

The Tl-based superconductor has a relatively high transition temperature compared with other cuprates [1]. It consists of several phases with different number of CuO and TlO layers. Among the phases, the $TlSr_2CaCu_2O_7$ (Tl-1212) is the most interesting in terms of superconducting phase formation. The Tl-1212 phase has a structure similar to $YBa_2Cu_3O_7$ (Y123) superconductor [2]. The Tl-1212 superconducting phase was reported by Halder et al. [3] in the $(Tl,Bi)Sr_2Ca_2CuO_7$ and by Parkin et al. [4] in the $TlBa_2CaCu_2O_7$. The $TlSr_2CaCu_2O_7$ was reported to be superconducting at about 80 K [5] but the phase is difficult to synthesize in pure form due to high average Cu valence [6]. Fortunately, the Tl-1212 phase can be stabilized by controlling the hole carrier concentration using partial substitution of various elements at the Ca, Sr and Tl sites to reduce the average Cu valence [7].

Superconductivity can be optimized for maximum transition temperature, T_c by reducing the average Cu valence to between +2.20 and +2.30 [8].

Several factors affect the formation of the Tl-1212 crystal structure. The ionic radius of the replaced or substituted elements can play an important role in the formation of the superconducting phase [9]. Substitution with metallic elements of higher valences decreases the formal valence of Cu, improves the superconducting properties and stabilizes the Tl-1212 phase. Partial replacement of Tl^{3+} by Bi^{3+}, Pb^{4+} and Cr^{3+} facilitates the formation of the Tl-1212 phase [10-12]. Substitution of rare-earth elements (RE) into the Sr^{2+} [13] and Ca^{2+} sites [14] can also facilitate the formation of the Tl-1212 phase. $TlSr_2(Ca,RE)Cu_2O_7$ with transition temperature of 90 K has been reported [15].

Substitutions of Cr for Tl or Ca sites stabilize the Tl-1212 phase and improve T_c to above 100 K [16]. Cr substituted $TlSr_2CaCu_2O_7$ samples were also successfully prepared using the co-precipitation method [17]. Cr in the Tl-1212 phase was suggested to be in the +3 state. Alkali metals (Na and Rb) with Cr substitutions in Tl-1212 phase improved the transition temperature [18]. An optimum Cu valence between +2.20 and +2.30 exhibits the maximum transition temperature in this phase [8, 19], which is consistent with the optimum value in the Y123 compound [20]. The effects of Ta-substitution at the Sr site have been reported with $T_{c\text{-onset}}$ of 90 K for $x = 0.1$ [21]. Elemental substitutions and additions are some of the techniques used to improve the superconducting properties of the high T_c cuprates [22, 23].

In this paper we have investigated the effects of transition metal, M = Rh and Ta on $Tl_{0.85}Cr_{0.15}Sr_{2-x}M_xCaCu_2O_7$ for $x = 0$–0.04 (M = Rh) and for $x = 0$–0.30 (M = Ta). Both the transition metal, Rh and Ta are multivalent with similar valence state of $Rh^{3+}/Rh^{4+}/Rh^{5+}$ and $Ta^{3+}/Ta^{4+}/Ta^{5+}$. The ionic radius with coordination number 6 of both transition metal overlaps, i.e. $Rh^{3+/4+/5+}$ (0.55 to 0.665 Å) and $Ta^{3+/4+/5+}$ (0.64 to 0.72 Å) and the ionic radius of Sr^{2+} is 1.18 Å [24]. It is interesting to investigate the effects of multivalent Rh and Ta at the Sr-site of the Tl-1212 phase. X-ray diffraction, scanning electron microscopy (SEM), DC electrical resistance and AC susceptibility results are reported. Our results showed that Rh and Ta improved the transition temperature of the $Tl_{0.85}Cr_{0.15}Sr_{2-x}M_xCaCu_2O_7$ phase from 97 K to 103 K and 104 K, respectively.

2. EXPERIMENTAL DETAILS

The solid-state reaction method with starting composition $Tl_{0.85}Cr_{0.15}Sr_{2-x}M_xCaCu_2O_7$ for $x = 0 – 0.04$ (M = Rh) and $x = 0 – 0.30$ (M = Ta) was used for samples preparation. High purity (99.9+%) powders of $SrCO_3$ (or SrO), CaO (or $CaCO_3$), CuO, Rh_2O_3 and Ta_2O_5 were ground and heated in air at 900 °C for 24 h. The furnace was naturally cooled. Then the powders were reground and reheated several times. Tl_2O_3 and Cr_2O_3 were then added to the precursor and mixed completely. In order to compensate for thallium loss during heating, excess 10% of $Tl2O_3$ was added. Pellets with 13 mm diameter and 2 mm thickness were made and heated in a tube furnace at 1000 °C in flowing O_2 for 4 min and furnace cooled to 300 K.

Powder X-ray diffraction measurement was performed using a Bruker D8 Advance diffractometer with CuK_α source. The volume fractions of the Tl-1212:1201:$Ca_{0.3}Sr_{0.7}CuO_2$ (CSCO) phases were estimated by using the formula:

$$\text{Tl-1212 \%} = \frac{\sum I_{Tl-1212}}{\sum I_{Tl-1212} + \sum I_{Tl-1201} + \sum I_{CSCO}} \times 100\%$$

$$\text{Tl-1201 \%} = \frac{\sum I_{Tl-1201}}{\sum I_{Tl-1212} + \sum I_{Tl-1201} + \sum I_{CSCO}} \times 100\%$$

$$\text{CSCO \%} = \frac{\sum I_{CSCO}}{\sum I_{Tl-1212} + \sum I_{Tl-1201} + \sum I_{CSCO}} \times 100\%$$

where $\sum I$ is the sum of intensity of each phase.

At least ten diffraction peaks were employed to calculate the lattice parameters of the Tl-1212 phase using the least squares fitting method. A Merlin Gemini microscope was used to record the microstructure.

The four-probe technique with constant current source between 1 and 100 mA was used to determine the electrical resistance at low temperature. Silver paste was used as electrical contacts. A closed cycle refrigerator from CTI Cryogenics Model 2 and a temperature controller from Lake Shore Model 330 were employed. A Cryo Industry AC susceptometer model number REF-1808-ACS was used to measure the susceptibility (frequency 295 Hz and field 5 Oe). The samples were cut into a bar shape for the measurements.

3. RESULTS AND DISCUSSION

Figures 1(a) and 1(b) show the XRD patterns of $Tl_{0.85}Cr_{0.15}Sr_{2-x}Rh_xCaCu_2O_7$ ($x = 0$, 0.01, 0.02 and 0.04). The patterns indicated a dominant Tl-1212 phase for $x = 0.01$ with $TlSr_2CuO_5$ (Tl-1201) and CSCO as minor phases. The Tl-1212 peaks can be indexed based on a tetragonal unit cell with space group, P4/mmm. Reflection peaks due to Tl-1201 are indicated with asterisks while reflection peaks due to CSCO are indicated in parentheses. Samples with nominal starting compositions $Tl_{0.85}Cr_{0.15}Sr_{2-x}Ta_xCaCu_2O_7$ also showed a multiphase of Tl-1212, Tl-1201 and CSCO (Figure 2). The XRD patterns of $x = 0$ and 0.1 indicated a dominant Tl-1212 phase. The CSCO impurity peaks were observed in all samples. Earlier studies also reported (Ca,Sr)CuO as a minor phase in $Bi_2Sr_2Ca_2Cu_3O_{10}$ [25] and $Bi_2Sr_2CaCu_2O_8$ [26] superconductors. It is interesting to note that in this work $Ca_{0.3}Sr_{0.7}CuO_2$ phase with orthorhombic structure (space group Cmcm (63)) was also found in the Tl-1212 superconductor.

The *c*-lattice parameter decreased with increase in Rh. The lattice parameters of the Tl-1212 phase for Rh ($x = 0.01$) samples were $a = 3.824$ Å and $c = 12.09$ Å and for Rh ($x = 0.02$), $a = 3.836$ Å and $c = 11.96$ Å. This decrease in the *c*-lattice parameter may be due to the smaller Rh ions replacing the larger Sr ion sites. In the Ta series, the lattice parameters for $x = 0.10$ samples were $a = 3.824$ Å and $c = 12.06$ Å, and for 0.20 samples, $a = 3.804$ Å and $c = 12.10$ Å. As the amount of Ta was increased, the *a*-lattice parameter decreased while the *c*-lattice parameter increased.

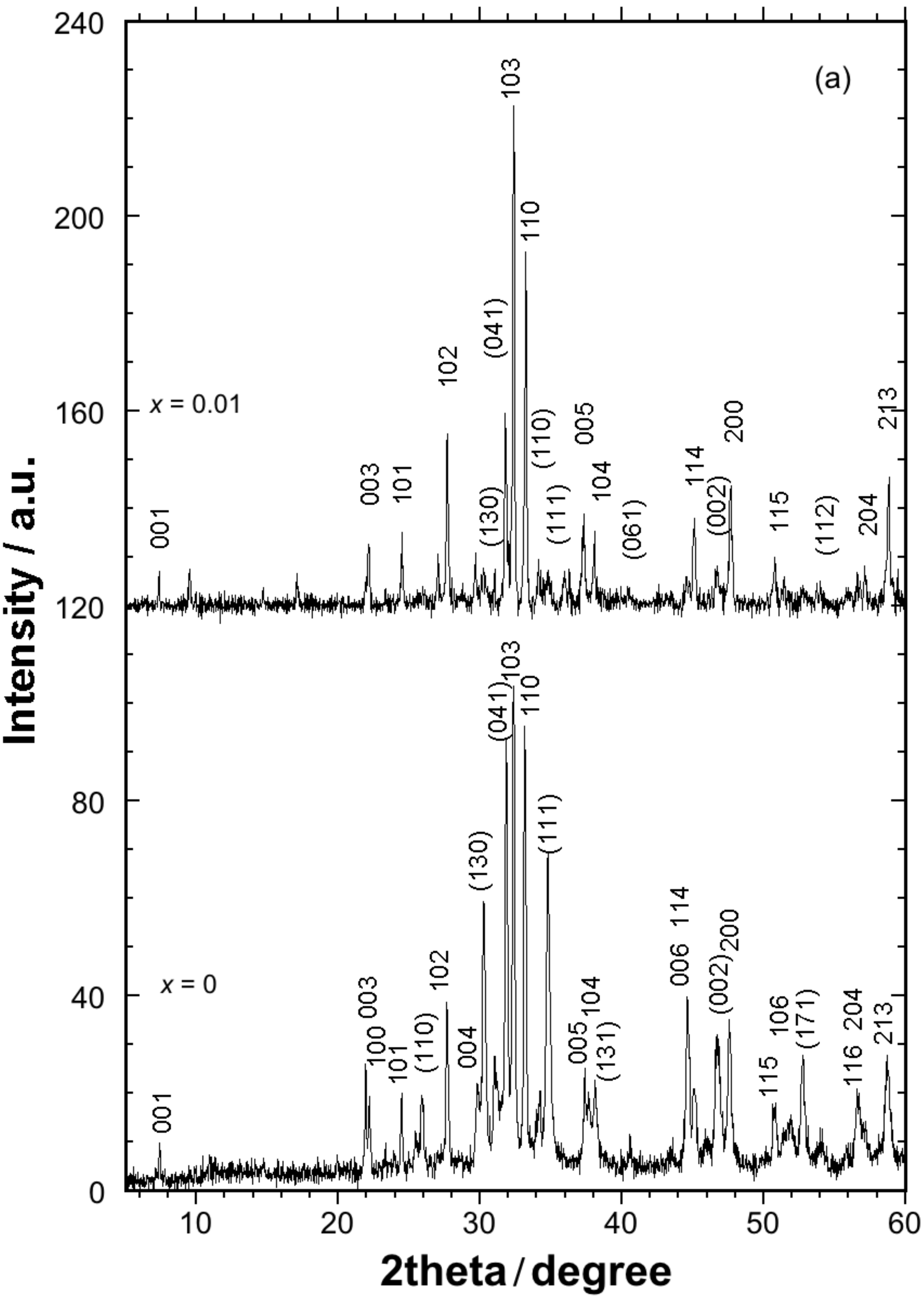
(a)
Intensity / a.u.
2theta / degree
x = 0.01
x = 0
0
40
80
120
160
200
240
10
20
30
40
50
60
001
003
101
102
(130)
(041)
103
110
(110)
(111)
005
104
(061)
114
(002)
200
115
(112)
204
213
001
100
003
101
(110)
102
004
(130)
(041)
103
110
(111)
005
104
(131)
006
114
(002)
200
115
106
(171)
116
204
213

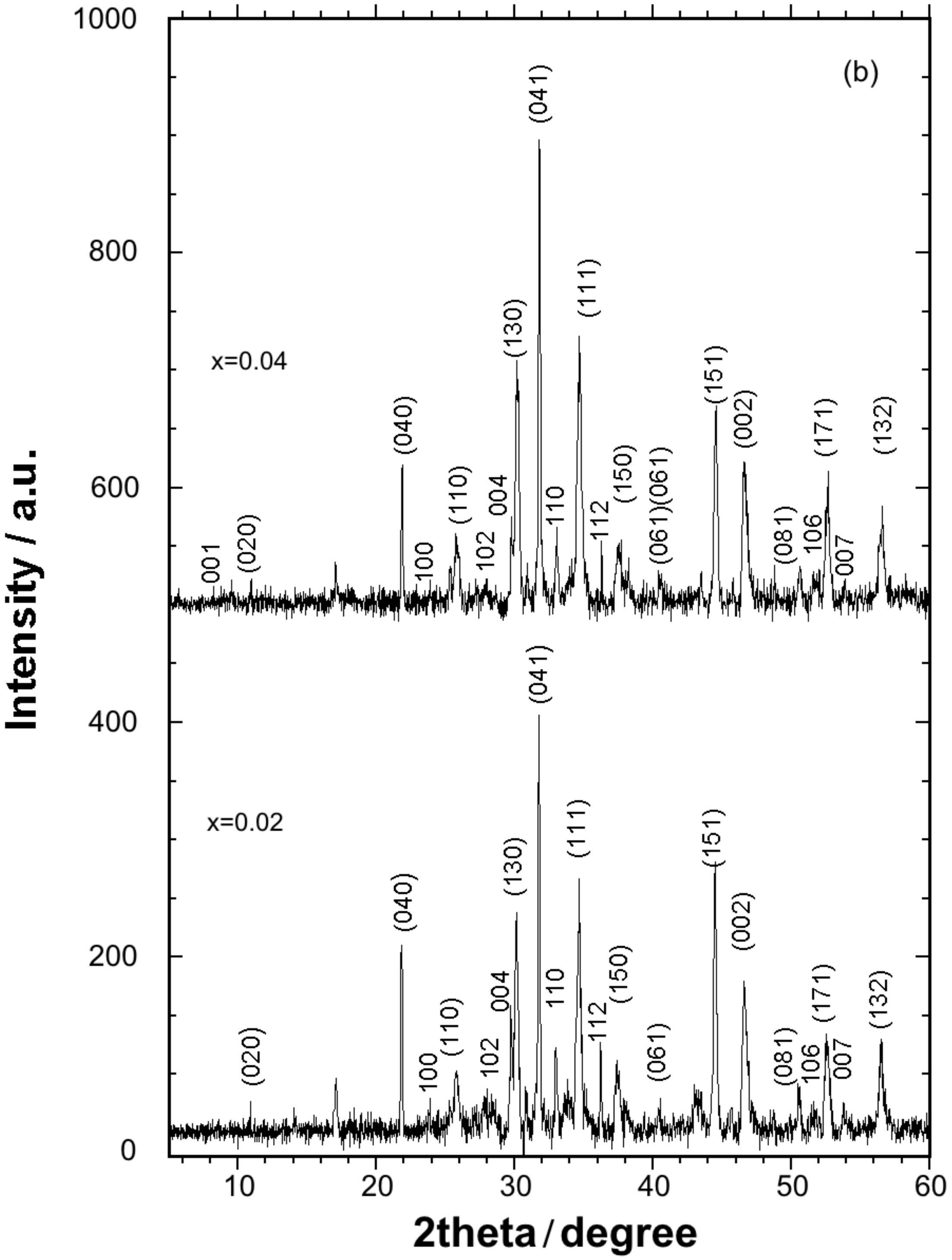

Figure 1. Powder X-ray diffraction patterns of samples with nominal starting composition $Tl_{0.85}Cr_{0.15}Sr_{2-x}Rh_xCaCu_2O_7$ for (a) $x = 0$ and 0.01, and (b) $x = 0.02$ and 0.04. Reflection peaks due to the 1201 phase are indicated in parentheses while reflection peaks due to the CSCO phase are indicated with asterisks.

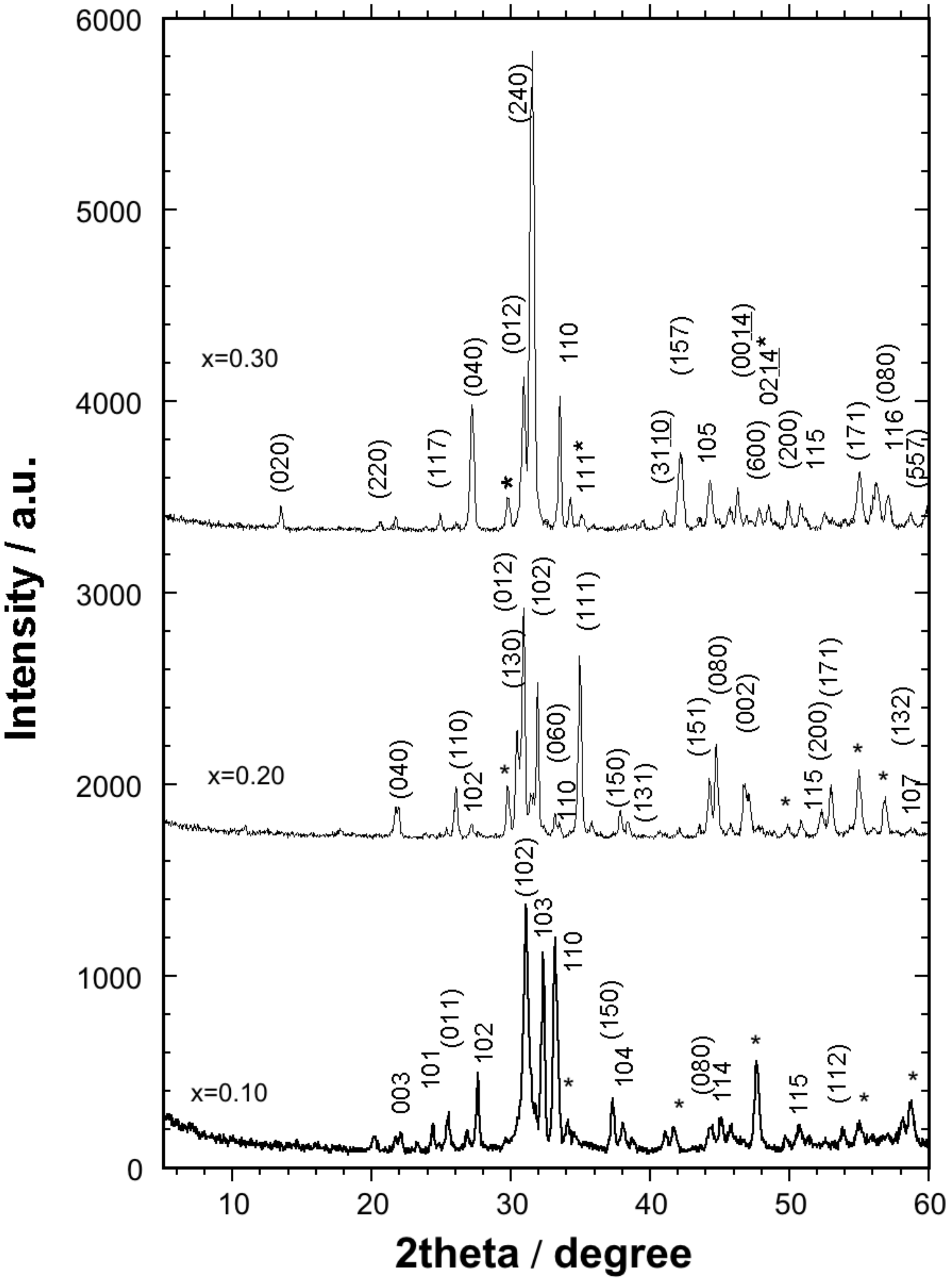

Figure 2. Powder X-ray diffraction patterns of samples with nominal starting composition $Tl_{0.85}Cr_{0.15}Sr_{2-x}Ta_xCaCu_2O_7$ for $x = 0.1$, 0.2 and 0.3. Reflection peaks due to the 1201 phase are indicated in parentheses while reflection peaks due to the CSCO phase are indicated with asterisks.

The powder X-ray diffraction patterns of both series showed that the amount of Tl-1212 phase reached a maximum when $x = 0.01$ for Rh and $x = 0.10$ for Ta. The XRD patterns showed that Rh samples have a higher amount of Tl-1212 phase compared to the Ta-substituted samples. Higher amounts of Rh and Ta resulted in an increase in the CSCO phase for $x > 0.01$ for Rh and $x > 0.10$ for Ta. This may be due to the ion size effect because Sr^{2+} (1.18 Å) is much larger than Rh^{3+} (0.665 Å) and Ta^{3+} (0.72 Å) where only a low concentration of these smaller ions can stabilize the Tl-1212 phase. Some Rh and Ta may also be substituted at the Ca site.

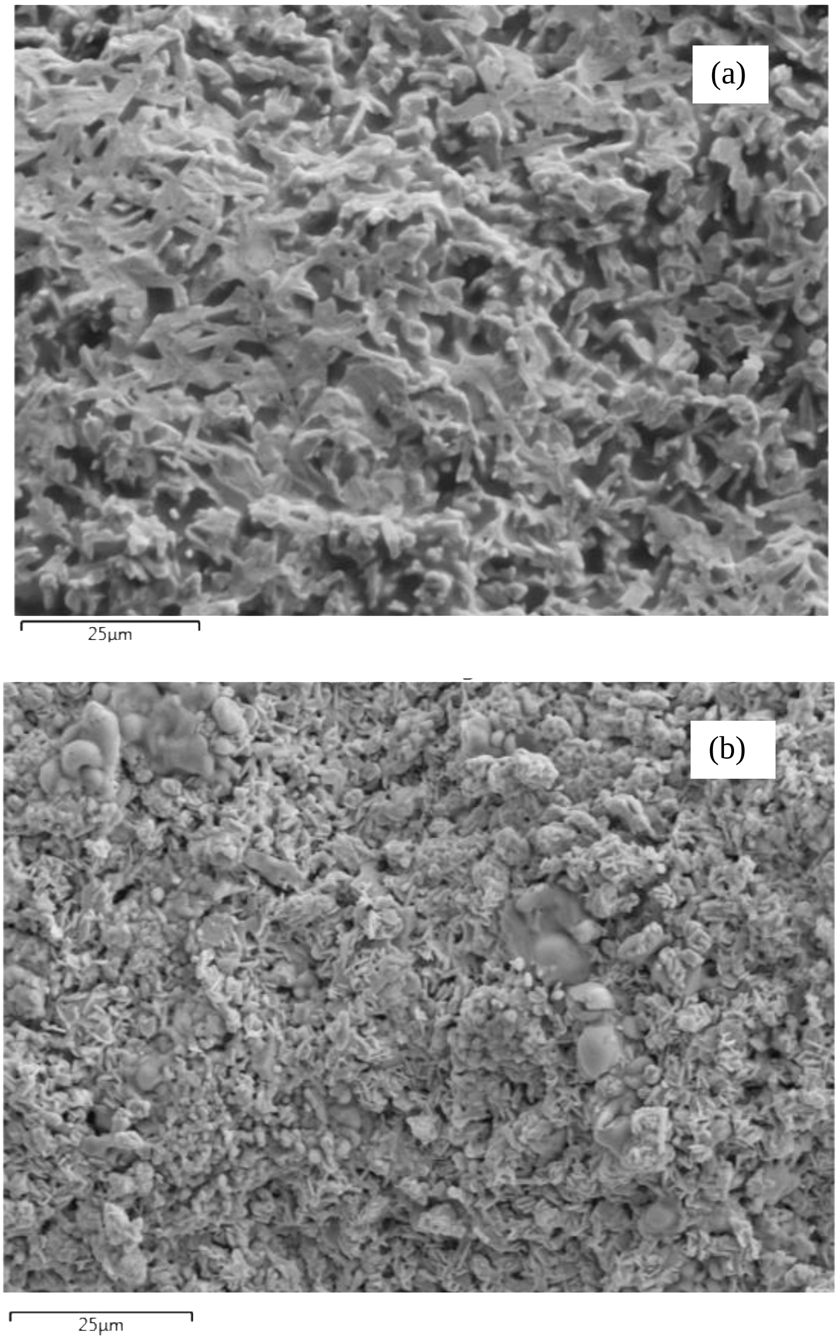

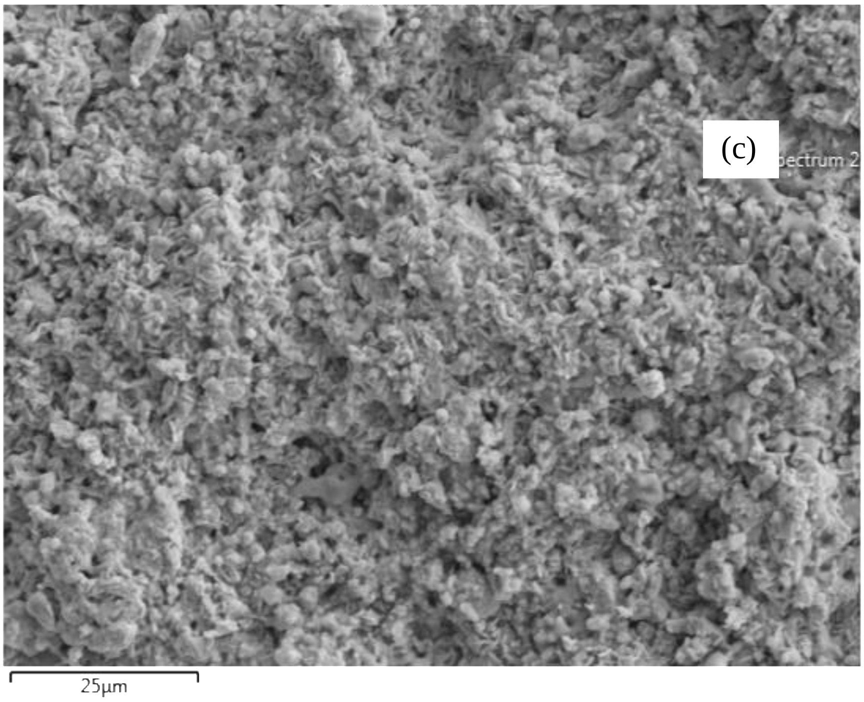

Figure 3. SEM micrographs of $Tl_{0.85}Cr_{0.15}Sr_{2-x}Rh_xCaCu_2O_7$ for (a) $x = 0.01$, (b) $x = 0.02$, (c) $x = 0.04$

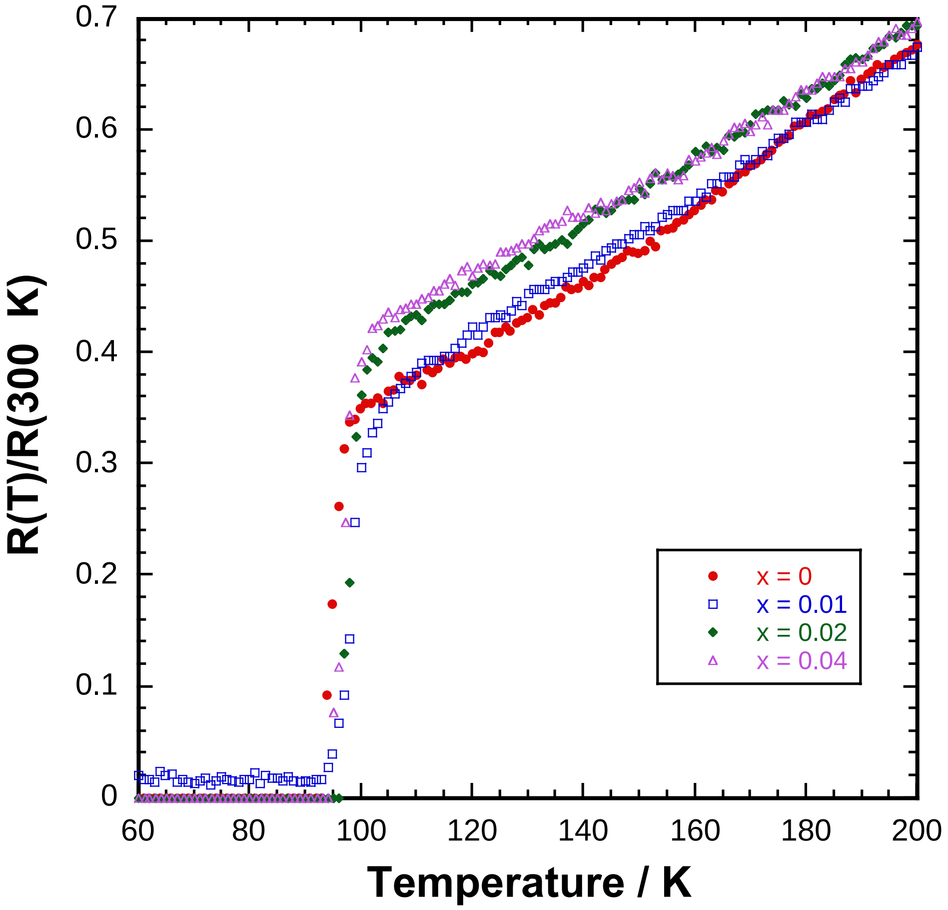

Figure 4. Normalized electrical resistance versus temperature for $Tl_{0.85}Cr_{0.15}Sr_{2-x}Rh_xCaCu_2O_7$ ($x = 0 – 0.04$)

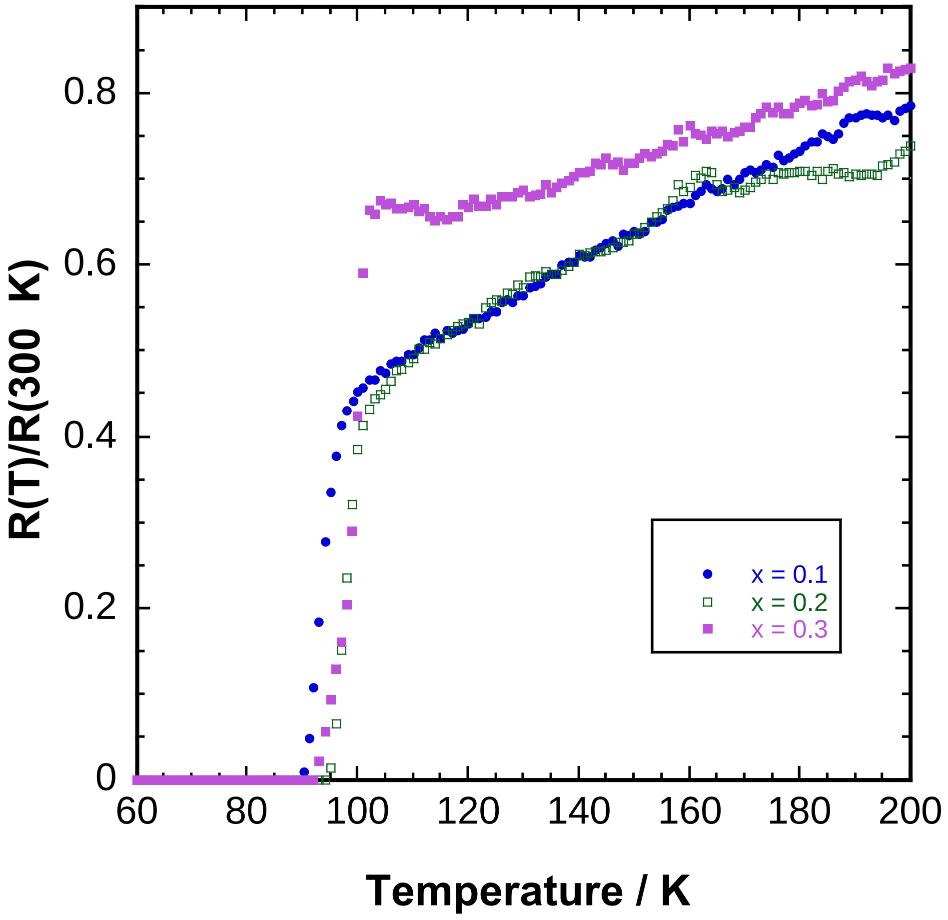

Figure 5. Normalized electrical resistance versus temperature for $Tl_{0.85}Cr_{0.15}Sr_{2-x}Ta_xCaCu_2O_7$ (x = 0.1 – 0.30)

SEM micrographs showed that the grain size decreased with substitution of Rh. For example Figure 3 shows the SEM micrographs of x = 0.01, 0.02 and 0.04 for Rh samples where a decrease in grain size was observed. The micrographs showed porous microstructure and irregularly shaped grains. Among the samples, the finest grain was observed for x = 0.04 while the x = 0.01 showed the largest grain size.

Figure 4 shows the temperature dependence of the resistance of $Tl_{0.85}Cr_{0.15}Sr_{2-x}Rh_xCaCu_2O_7$ samples. $Tl_{0.85}Cr_{0.15}Sr_2CaCu_2O_7$ was observed to superconduct with $T_{c\text{-onset}}$ of 97 K and $T_{c\text{-zero}}$ of 93 K. Samples of Rh with x = 0.01 showed $T_{c\text{-onset}}$ increased to 103 K. Further increase in Rh content also improved $T_{c\text{-zero}}$ to 96 K (x = 0.02) and 94 K (x = 0.04). The resistance-temperature measurements showed metallic normal state behavior for all samples. Room-temperature resistivity increased from 0.657 mΩ.cm for x = 0 to 1.719 mΩ.cm for x = 0.01 and 1.44 mΩ.cm for x = 0.04 (Table 1).

Figure 5 shows the electrical resistance versus temperature curves for $Tl_{0.85}Cr_{0.15}Sr_{2-x}Ta_xCaCu_2O_7$. $T_{c\text{-onset}}$ and $T_{c\text{-zero}}$ were higher than the non Ta-substituted samples. The highest transition temperature was exhibited by x = 0.20 with $T_{c\text{-zero}}$ of 91 K. The room-temperature resistivity generally increased with Ta content. $T_{c\text{-onset}}$ and $T_{c\text{-zero}}$, room-temperature resistivity at 300 K and volume fraction of Rh and Ta substituted samples are shown in Tables 1 and 2, respectively.

Table 1. $T_{c\text{-onset}}$, $T_{c\text{-zero}}$, $T_{c\chi'}$, T_p, room temperature resistivity, major and minor phase in $Tl_{0.85}Cr_{0.15}Sr_{2-x}Rh_xCaCu_2O_7$

x	$T_{c\text{-onset}}$ / K	$T_{c\text{-zero}}$ / K	$T_{c\chi'}$ / K	T_p / K	$\rho_{300\text{ K}}$ (mΩ.cm)	Phase Major : Minor
0	97	93	94	68	0.657	Tl-1212 : CSCO
0.01	103	93	97	88	1.72	Tl-1212 : CSCO/Tl-1201
0.02	102	96	98	93	0.927	CSCO : Tl-1212/Tl-1201
0.04	101	94	95	90	1.44	CSCO : Tl-1212/Tl-1201

Table 2. $T_{c\text{-onset}}$, $T_{c\text{-zero}}$, $T_{c\chi'}$, T_p, room temperature resistivity, major and minor phase in $Tl_{0.85}Cr_{0.15}Sr_{2-x}Ta_xCaCu_2O_7$

x	$T_{c\text{-onset}}$ / K	$T_{c\text{-zero}}$ / K	$T_{c\chi'}$ / K	T_p / K	$\rho_{300\text{ K}}$ (mΩ.cm)	Phase Major : Minor
0.10	102	88	88	86	2.064	Tl-1212 : CSCO/Tl-1201
0.20	104	91	53	45	0.660	CSCO : Tl-1212/Tl-1201
0.30	103	90	96	91	6.078	CSCO : Tl-1212/Tl-1201

The increase in *c*-lattice with increasing Ta may be explained in terms of average Cu valence concept [8, 19]. The CuO plane determines the *c*-lattice where substitution of Ta ion with a higher valence for Sr^{2+} decreases the average Cu valence and caused the conversion from Cu^{3+} to larger Cu^{2+}. This conversion resulted in an increase in the Cu-O distance causing the *c*-lattice to expand. The Ta substituted sample for $x = 0.20$ showed the highest increase in $T_{c\text{-onset}}$ and $T_{c\text{-zero}}$. This indicated that the doping level of the Tl-1212 phase was optimal at $x = 0.2$. The slight improvement in the transition temperature for low substitution levels is similar to alkali metals (Na and Rb) with Cr substitutions in the Tl-1212 phase [18]. Table 3 shows the transition temperature of various elemental substitutions into the Tl-1212 phase. Incorporation of Cr with Ta and Rh increased the transition temperature of the Tl-1212 phase to values higher than Se, V and Zr substitutions

From AC susceptibility, the transition temperature was determined from the sudden decrease in the real part of the susceptibility χ. The peak temperature (T_p) in the imaginary part of the susceptibility χ'' represents the AC losses. $T_{c\chi'}$ was between 95 and 98 K for Rh samples (Figure 6) and between 53 and 96 K for Ta-substituted samples (Figure 7).

The $x = 0.01$ and 0.02 Rh samples showed a slight increase in $T_{c\chi'}$. T_p generally increased with Rh, which was due to the increased in inter-grain coupling from the larger grain size (Figure 3). Two loss peaks were observed in the Rh sample with $x = 0.02$ and $x = 0.04$ as shown in Figure 6 which include a broadening of T_p at low temperatures as a result of coupling losses and a narrower peak due to intrinsic losses at higher temperatures near $T_{c\chi'}$. $T_{c\chi'}$ of the Rh sample, shifted to lower temperatures from 91 K (x = 0) to 88 K (x = 0.01) indicating a weaker pinning force strength. T_p of Rh samples recorded a maximum value of 93 K for x = 0.02 indicating a stronger pinning force strength. For Ta substituted samples, T_p showed maximum value of 91 K for x = 0.30 indicating the strongest pinning force strength and the lowest value of 45 K for x = 0.20 showing a weak pinning force strength. The low $T_{c\chi'}$ and T_p for x = 0.2 may be due to the impurities specific to this sample. $T_{c\chi'}$ for Rh samples was higher than Ta substituted samples.

Table 3. Elemental substitution in $TlSr_2CaCu_2O_7$ system

Elements				T_c / K		
Ion	Valence State	Ionic Radius (6 CN) / Å	Composition	$T_{c\ onset}$	$T_{c\ zero}$	Ref.
			$TlSr_2CaCu_2O_7$	ns		[27]
					47	[28]
Ta	+3 +4 +5	0.72 0.68 0.64	$(Tl_{0.85}Cr_{0.15})Sr_{2-x}Ta_xCaCu_2O_7$	104	91	This work
Rh	+3 +4 +5	0.665 0.60 0.55	$(Tl_{0.85}Cr_{0.15})Sr_{2-x}Rh_xCaCu_2O_7$	103	93	This work
Se	+6 +4	0.56 0.64	$(Tl_{0.6}Se_{0.4})Sr_2CaCu_2O_7$	76	67	[27]
Cr	+6 +5 +4 +3 +2	0.58 0.63 0.69 0.755 0.94	$(Tl_{0.5}Cr_{0.5})Sr_2CaCu_2O_7$	110	102	[16]
V	+5 +4 +3 +2	0.68 0.72 0.78 0.93	$(Tl_{0.50}V_{0.50})Sr_2CaCu_2O_7$	80	57	[29]
Zr	+4	0.86	$(Tl_{0.8}Zr_{0.2})Sr_2CaCu_2O_7$	84		[30]

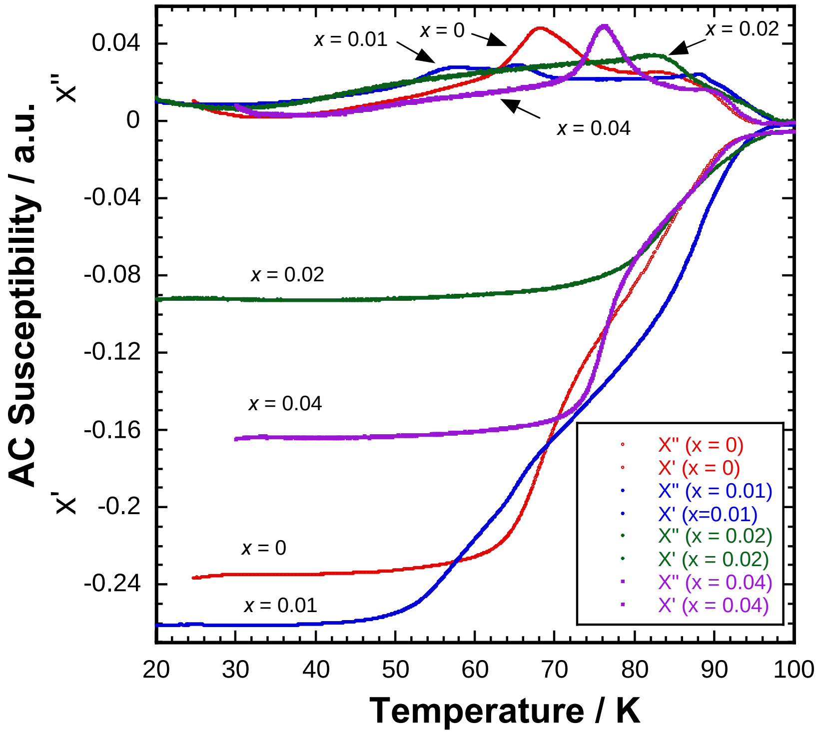

Figure 6. AC susceptibility ($\chi = \chi' + i\chi''$) versus temperature of $Tl_{0.85}Cr_{0.15}Sr_{2-x}Rh_xCaCu_2O_7$ (x = 0, 0.01, 0.02, 0.04)

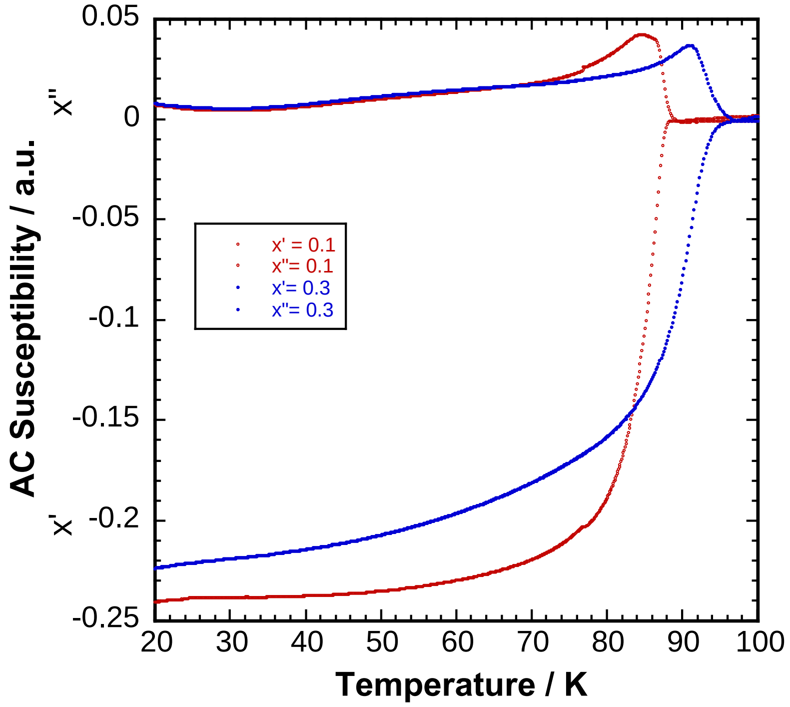

Figure 7. AC susceptibility ($\chi = \chi' + i\chi''$) versus temperature of $Tl_{0.85}Cr_{0.15}Sr_{2-x}Ta_xCaCu_2O_7$ (x = 0.10, 0.20, 0.30)

In conclusion, the effects of transition metal M = Rh and Ta on $Tl_{0.85}Cr_{0.15}Sr_{2-x}M_xCaCu_2O_7$ have been investigated. The results showed the formation of Tl-1212 and other impurity phases. Rh samples have a higher amount of Tl-1212 phase compared with the Ta-substituted samples. Transition metal with smaller ionic radius showed suppressed flux pinning and weak inter-granular coupling. These results showed that Rh stabilized the Tl-1212 phase better than Ta. The optimal sintering procedure to obtain higher quality samples can be determine for further works. In addition, the effect of Rh, Ta and other transition metal on the properties of Tl-1212 phase with Bi and Pb for example, $(Tl_,Pb/Bi)Sr_{2-x}M_xCaCu_2O_7$ can be performed to investigate further the effects of transition metal on this superconductor.

ACKNOWLEDGEMENTS
The authors thank the Ministry of Education of Malaysia for funding this project (grant no. FRGS/1/2017/STG02/UKM/01/1).

CONFLICT OF INTEREST
We declare no conflict of interest.

References

1. Z. Z. Sheng and A. M. Hermann, *Nature*, 332 (1998) 138.
2. S. Nakajima, M. Kikuchi, Y. Syono, N. Kobayashi and Y. Muto, *Phys. C,* 168 (1990) 57.
3. S. Hadlar, S. Sridhar, A. Roig-Janicki, W. Kennedy, D. H. Wu, C. Zahopoulos and B. C. Giessen, *J. Supercond.*, 1 (1988) 211.
4. S. S. P. Parkin, V. Y. Lee, A. I. Nazzal, R. Savoy, R. Beyers and S. J. Laplaca, *Phys. Rev. Lett.*, 61 (1988) 750.
5. M. A. Subramanian, J. C. Calabrese, C. C. Torardi, J. Gopalakrishnan, T. R. Askew, R. B. Flippen, K. J. Morrissey, U. Chowdhry and A. W. Sleight, *Nature,* 332 (1988) 420.
6. M.A. Subramanian, C.C. Torardi, J. Gopalakrishnan, P.L. Gai, J.C. Calabrese, T.R. Askew, R.B. Flippen and A.M. Sleight, *Science*, 242 (1988) 249.
7. R.S. Liu, W. Zhou, R. Janes and P.P. Edwards, *Supercond. Sci. Technol.*, 4 (1991) 310.
8. Z.Z. Sheng, Y. Xin, D.X. Gu, J.M. Meason, J. Bennett, D. Ford and P.O. Pederson, *Phys. B,* 84 (1991) 349.
9. K. Muhammad-Aizat and R. Abd-Shukor, *Sains Malaysiana*, 47 (2018) 1579.
10. Y.F. Lee, O. Chmaissem and Z. Z. Sheng, *Phys. C*, 248 (1995) 42.
11. M. G. Ranjbar Ghazeian, Mahmood Ghoranneviss and R. Abd-Shukor, *Appl. Phys. A,* 124 (2018) 456.
12. S.S.O. Farhat and R. Abd-Shukor, *Int. J. Electrochem. Sci.*, 13 (2018) 7846.
13. W. H. Lee and B. C. Huang, *Phys. C***,** 289 (1997) 114.
14. Y. Xin, Y. F. Lee, D. Ford, D. O. Pederson and Z. Z. Shen, *Jpn J. Appl. Phys.,* 30 (9A) (1991) L1549.
15. I. B. Parise, P. I. Gai, M. A. Subramanian, J. Gopalakrishnan and A. W. Sleight, *Phys. C*, 159 (1989) 245.
16. Z. Z. Sheng, D. X. Gu, Y. Xin, D. O. Pederson, L. W. Finger, C. G. Hadidiacos and R. M. Hazen, *Mod. Phys. Lett. B*, 9 (1991) 635.
17. I. Hamadneh, Y. K. Kuan, L. T. Hui and R. Abd-Shukor, *Mater. Lett.*, 60 (2006) 734.

18. J. Nur-Akasyah and R. Abd-Shukor, *J. Mater. Sci.: Mater. in Electron.*, 29(5) (2018) 3690.
19. Ilhamsyah Putra Abu Bakar and R. Abd-Shukor, *J. Alloys Compd.*, 772 (2019) 745.
20. S. Nakajima, M. Kikuchi, Y. Syono, N. Kobayashi and Y. Muto, *Phys. C*, 168 (1990) 57.
21. A.K. Yahya, M.I. Yusof, B. Musa, W.F. Abdullah, Z. Zamri and M.H. Jumali, *J. Appl. Sci.,* 8 (2008) 1007.
22. Y. Slimani, E. Hannachi, A. Ekicibil, M.A. Almessiere and F. Ben Azzouz, *J. Alloys Compd.,* 781 (2019) 664.
23. Y. Slimani, M.A. Almessiere, E. Hannachi, M. Mumtaz, A. Manikandan, A. Baykal and F. Ben Azzouz, *Ceram. Int.,* 45 (2019) 6828.
24. R. D. Shannon, *Acta Cryst. A,* 32 (1976) 751.
25. B. Özkurt, *J. Mater. Sci.: Mater. Electron.*, 25 (2014) 3295.
26. B. Özçelik, O. Nane, A. Sotelo, H. Amaveda and M.A. Madre, *J. Mater. Sci.: Mater. Electron.,* 28 (2017) 6278.
27. J. Nur-Akasyah and R. Abd-Shukor, *Cryogenics,* 100 (2019) 109.
28. C. Martin, J. Provost, D. Bourgalt, B. Domenges, C. Michel and M. Hervieu, *Phys. C,* 157 (1989) 460.
29. R. S. Liu, W. Zhou, R. Janes and P. P. Edwards, *Solid State Commun.,* 76 (1990) 1261.
30. R. Abd-Shukor and K. H. Lee, *J. Mater. Sci.: Mater. Electron.,* 9 (1998) 99.